SUPPLEMENTAL MATERIAL

Abnormal lymphatic S1P signaling aggravates lymphatic dysfunction and tissue inflammation

Dongeon Kim, PhD [1,2,#], Wen Tian, PhD [1,2,#], Timothy Ting-Hsuan Wu, MS [2,3], Menglan Xiang, PhD [1,2], Ryan Vinh, BS [1,2], Jason Lon Chang, BS [1,2], Shenbiao Gu, BS [1,2], Seunghee Lee, PhD [1,2], Yu Zhu, PhD [1,2], Torrey Guan, BS [1,2], Emilie Claire Schneider, MS [1,2], Evan Bao, MS [1,2], J. Brandon Dixon, PhD [4], Peter Kao, MD [2], Junliang Pan, PhD [1,2], Stanley G. Rockson, MD [2], Xinguo Jiang, MD, PhD [1,2,*], and Mark Robert Nicolls, MD [1,2,*].

[1]VA Palo Alto Health Care System, Palo Alto, California, USA.
[2]Stanford University School of Medicine, Stanford, California, USA.
[3]Department of Biochemistry, Stanford Bio-X, Stanford, California, USA.
[4]Georgia Institute of Technology, Atlanta, Georgia, USA

# These authors contributed equally to this work
*To whom correspondence may be addressed. E-mail: mnicolls@stanford.edu; xinguoj@stanford.edu

Table S1. Demographics of controls and lymphedema patients used for S1P analysis

Patient ID	Age	Sex	BMI	ISL Class (1-3)	Primary / Secondary	Duration of Disease (year)	S1P LC-MS/MS (pg/ml)
C1	33	M	n/a	n/a	n/a	n/a	686.0
C2	35	M	n/a	n/a	n/a	n/a	511.0
C3	30	F	n/a	n/a	n/a	n/a	475.0
C4	21	M	n/a	n/a	n/a	n/a	444.0
C5	31	M	n/a	n/a	n/a	n/a	412.0
C6	32	M	n/a	n/a	n/a	n/a	404.0
C7	27	F	n/a	n/a	n/a	n/a	363.0
C8	60	M	n/a	n/a	n/a	n/a	360.0
C9	61	M	n/a	n/a	n/a	n/a	351.0
C10	84	M	n/a	n/a	n/a	n/a	254.0
P1	68	F	26.19	2	Secondary	4	200.0
P2	85	F	26.18	2	Secondary	4	193.0
P3	44	F	24.58	2	Secondary	38	185.0
P4	27	M	22.97	2	Primary	8	182.0
P5	62	F	33.08	2	Secondary	5	172.0
P6	59	F	29.27	2	Secondary	22	142.0
P7	77	F	37.68	2	Secondary	5	100.0
P8	76	F	48.53	3	Primary	childhood	85.0
P9	69	M	51.35	2	Secondary	13	72.0
P10	71	F	23.67	2	Secondary	4	46.0

C1-C10 represents healthy control.
P1-P10 belongs to the lymphedema cohort.
n/a, not applicable

BMI= Body mass index
ISL= International Society of Lymphology

Table S2. Clinical Characteristics and S1P serum levels for lymphedema subjects and healthy control

	Health control	Lymphedema cohort	P value
Age (years)	41 ± 20	64 ± 17	P<0.02
Female sex - no. (%)	2 (80)	8 (80)	P=0.008
BMI	N/A	32 ± 10	
Lymphedema ISL Class 2 (%)	N/A	90	
Lymphedema ISL Class 3 (%)	N/A	10	
Primary Lymphedema (%)	N/A	20	
Secondary Lymphedema (%)	N/A	80	
Disease duration (years)	N/A	18 ± 23	

The dichotomous variables were statistically analyzed with Chi Square test, the continuous variables with unpaired t test, and numerical data are presented with mean plus/minus standard deviation.

Table S3. The sequences of the mouse-specific primers used for RT-qPCR

Gene (mouse)	Sense (5′→3′)	Antisense (5′→3′)
Sphk1	CGGTGATGGTCTGATGCATG	GAGGCTACACAGGGGTTTCT
S1pr1	GCCACCACTTACAAGCTCAC	CAAACATACTCCCTTCCCGCA
18s	GGACCAGAGCGAAAGCATTTGCC	TCAATCTCGGGTGGCTGAACGC

Table S4. The sequences of the human-specific primers used for RT-qPCR

Gene (human)	Sense (5′→3′)	Antisense (5′→3′)
S1PR1	TGCTGGCAAATTCAAGC	GGGTTGTCCCCTTCGTC
S1PR2	AAGCTGTATGGCAGCGA	AGAAGATGGTCACCACGCAC
S1PR3	TGGTCCCCACTCTTCATCCT	CAGCCAACACGATGAACCAC
S1PR4	CGTCTTTGGCTCCAACCTCT	TGCTGCGGAAGGAGTAGATG
S1PR5	CGCCTTCATCGTGCTAGAGA	CAGGAGCAGGAACATGGGA
SPHK1	GAGAAGTATCGGCGTCTGGG	CTACAGGGAGGTAGGCCAGT
SPHK2	CTGACTGGGAGGAAGCTGTG	AGTTGAGCAACAGGTCGAGG
18S	CTGCCATTAAGGGTGTTGGC	CAGCCCTCTGGTGGGTCAAT

Table S5. Key resources

REAGENT or RESOURCE	SOURCE	IDENTIFIER
Antibodies		
Anti-mouse-CD4 (GK 1.5), BV421	BD Bioscience	562891
Anti-mouse-CD8 (53-6.7), APC-Cy7	BD Bioscience	557654
Anti-mouse-CD25 (PC61), PE	BD Bioscience	553866
Anti-mouse-CD25 (PC61), BB700	BD Bioscience	566498
Anti-mouse-CD31 (MEC 13.3), BV421	BD Bioscience	562939
Anti-mouse-CD44 (IM7), PE-Cy7	BD Bioscience	560569
Anti-mouse-CD45 (30-F11), BB515	BD Bioscience	564590
Anti-mouse-CD69 (H1.2F3), BV650	BD Bioscience	740460
Anti-mouse-CD103 (2E7), BB700	BD Bioscience	748240
Anti-mouse-IFN-γ (XMG1.2), FITC	BD Bioscience	554411,
Anti-mouse-IL-4 (11B11), PE	BD Bioscience	554435,
Anti-mouse-IL-17A (TC11-18H10), AF647	BD Bioscience	560184
Anti-mouse-Foxp3 (R16-715), AF647	BD Bioscience	563486
Anti-mouse-S1PR1 (713412), APC	R&D systems	FAB7089A
IgG2A isotype (54447), APC	R&D systems	IC006A
Anti-mouse-podoplanin (gp38) (8.1.1), PE	BD Bioscience	566390
IgG2a,k isotype (G155-178), PE-CF594	BD Bioscience	562306
Anti-human-CD4 (OKT4), BV421	BD Bioscience	566703
Anti-human-CD8 (RPA-T8), BV480	BD Bioscience	566121
Anti-human-CD44 (G44-27), PE-Cy7	BD Bioscience	560533
Anti-human/mouse CLA (HECA-452), AF647	Biolegend	321310
Anti-human-IFN-γ (B27), FITC	BD Bioscience	554700
Anti-human-IL-4 (MP4-25D2), PE	BD Bioscience	554485

Anti-human-IL-17A (560490), AF647	BD Bioscience	560490
Monoclonal Rat anti-mouse LYVE1 (ALY7)	LSBio	LS-C106690
Monoclonal Mouse Anti-Human podoplanin (D2-40)	Dako	M3619
S1P1 Polyclonal Antibody	Invitrogen	PA1-1040
Recombinant Anti-CD4 antibody (EPR19514)	Abcam	Ab183685
Chemicals, Peptides, and Recombinant Proteins		
eBioscience Fixable Viability Dye eFluor 506	ThermoFisher	65-0866
eBioscience Fixable Viability Dye eFluor 780	ThermoFisher	65-0865
NA/LE anti-mouse CD3 (145-2C11)	BD Bioscience	553057
NA/LE anti-mouse CD28 (37.51)	BD Bioscience	553294
Purified Rat Anti-mouse CD16/CD32 (2.4G2)	BD Bioscience	553142
ImmunoCult™ Human CD3/CD28 T cell Activator	STEMCELL	10991
Cell Stimulation Cocktail (plus protein transport inhibitors) (500x)	Invitrogen	00-4975
Bovine Plasma Fibronectin (BPF)	ScienCell	8248
AbC Total Antibody Compensation Bead Kit	Invitrogen	A10497
Endothelial Cell Growth Medium 2 Kit	PromoCell	C-22111
Advanced RPMI 1640 Medium	Bibco	12633012
Penicillin-Streptomycin-Glutamine (100X)	Gibco	10378016
Trypsin-EDTA (0.25%), phenol red	Gibco	25200056
Ad-GFP-U6-h-S1PR1-shRNA	VECTOR BIOLABS	shADV-230289
4-deoxy Pyridoxine (4-DP)	Cayman	21863
Anti-mouse P-selectin Ab (RB40.34.4)	Make it in-house	
Anti-human P-selectin Ab (Waps 12.2)	Make it in-house	
Histopaque-1077 hybr-Max	Sigma	H8889
Normal Donkey Serum	Jackson Immu.Resear.	017-000-121
Antifade Mounting medium with DAPI	VECTOR	H-1200
Donkey anti-rat-Cy3	Jackson Immu.Resear.	712-166-150
Donkey anti-rat-AF488	Jackson Immu.Resear.	712-546-153
Donkey anti-rabbit-Cy3	Jackson Immu.Resear.	711-165-152
Indocyanine green (ICG)	MedChemExpress	HY-D0711
Tamoxifen	Sigma	T5648
Human Derma Lymphatic Endothelial Cells	PromoCell	C-12217
Buffy coat from whole blood	Stanford Blood Center	A1005
Critical Commercial Assays		
Naïve $CD4^+$ T cell Isolation Kit (mouse)	Miltenyi Biotec	130-104-453
Foxp3/Transcription Factor Staining Buffer Set	ThermoFisher	00-5523-00
Intracellular Fixation/Permeabilization Buffer Set	ThermoFisher	88-8824-00
Multi Tissue Dissociation Kit I	Miltenyi Biotec	130-110-201
EasySep Human Naïve $CD4^+$T cell Isolation Kit I	STEMCELL	19555
EasySep Human Naïve $CD4^+$T cell Isolation Kit II	STEMCELL	17555
EasySep Human Memory $CD4^+$T cell Isolation Kit	STEMCELL	19157
RNeasy® Plus Mini Kit	QIAGEN	74136
RNeasy® Mini Kit	QIAGEN	74106
RNeasy® Fibrous Tissue Mini Kit	QIAGEN	74704

Experimental Models: Organisms/Strains		
C57BL/6J	Jackson Laboratory	JAX:000664
Prox1tm3(cre/ERT2)Gco/J	Jackson Laboratory	JAX:022075
B6.129S6(FVB)-S1pr1tm2.1Rlp/J	Jackson Laboratory	JAX:019141
B6.Cg Gt(ROSA)26Sortm14(CAG-tdTomato)Hze/J	Jackson Laboratory	JAX:007914
Prox1-Cre^{ERT2}S1pr1$^{fl/fl}$ (*S1pr1*^{LECKO})	This paper	N/A
Prox1-Cre^{ERT2}-tdTomato	This paper	N/A
Software and Algorithms		
FACSAria III Sorter	BD Biosciences	
DMi8	LEICA	
LSR Fortessa	BD Biosciences	
LSM710	Zeiss	
D-520 Zoom digital camera	Olympus	
MVX10	Olympus	
AMI Prism® 7900HT Sequence Detection System	Appliedbiosystems	
MACS Octo Dissociator with Heaters	Miltenyi Biotec	
FlowJo (version 10)	BD Biosciences	
ImageJ		
Imaris	Oxford Instruments	
GraphPad Prism (version 9)	GraphPad	
JMP Pro 17	JMP	

Table S6. The list of differentially up-regulated gene in sh*S1PR1*-HDLECs

Without CD4 T cell co-culture	Intersection	With CD4 T cell co-culture			
STAB2	SELP	OMG	CPM	WDFY4	SLC12A5
AGTR1	RGS5	GPNMB	PCDH17	LIMCH1	COL12A1
TCF15	DIRAS3	BRME1	MMP9	CD36	KCNN4
MAILR	ADAMTS18	TOX	H2BC4	LFNG	ZC3H12A-DT
FLRT3	ADRA1D	KIF19	ADAMTS14	OLFM1	ADGRG4
RNF185-AS1	APLN	TIPARP-AS1	DRAXIN	DCLK1	TMEM163
PITX1-AS1	IL33	CEROX1	MYRIP	CETP	RPLP0P6
C3AR1		SPEG	CDH11	SIRT4	CORO2B
CFI		RPAP3-DT	CEND1	RASSF5	LINC02015
SPTBN5		TSPAN11	MIR210HG	SELE	CHST6
TGFA		SRGAP3	AR	H2AC6	HOXD3
		GOLGA8R	TRIM73	AQP11	ZNF667-AS1
		LINC01303	NEK10	COL9A3	INKA1
		LINC02159	TMEM265	LYPD1	LINC02154
		DUT-AS1	DPEP1	NPFFR2	MAP1A
		MAN1C1	PKIB	CTXN1	COL15A1
		ODAD3	NPTX2	PTGS1	PRND
		CPE	KCNE3	MAFB	SLCO2B1
		KIF1A	RN7SL3	ASS1	SORL1
		PTGIS	SLC22A17	CKB	PIK3R3

		GRM1	BMPER	SLC9A7	NPTXR
		MIR503HG	H2BC5	FOXD1	MARVELD3
		AIF1L	IL2RB	H2BC12	ZAP70
		PCDHB6	AFTPH-DT	ASRGL1	MYG1-AS1
		SOGA3	HSD17B14	CXADR	CPA4
		PCMTD1-DT	RNASE1	SELL	SNCB

Table S7. Fold change of differentially up-regulated gene in sh*S1PR1*-HDLECs.

Without CD4 T cell co-culture		**With CD4 T cell co-culture**					
Gene symbol	**Fold change**	**Gene symbol**	**Fold change**	**Gene symbol**	**Fold change**	**Gene symbol**	**Fold change**
STAB2	15.91	OMG	16.11	ADAMTS14	3.73	LINC02015	2.64
AGTR1	10.02	GPNMB	13.86	DRAXIN	3.70	SIRT4	2.59
SELP	9.97	BRME1	13.13	MYRIP	3.61	RASSF5	2.56
TCF15	9.44	TOX	12.46	CDH11	3.60	SELE	2.55
ADAMTS18	6.22	KIF19	10.25	CEND1	3.60	H2AC6	2.53
MAILR	6.21	TIPARP-AS1	9.66	DIRAS3	3.57	AQP11	2.53
FLRT3	5.86	SELP	9.36	MIR210HG	3.52	COL9A3	2.52
RNF185-AS1	4.40	CEROX1	9.09	AR	3.45	LYPD1	2.51
PITX1-AS1	3.38	SPEG	8.99	TRIM73	3.43	IL33	2.50
DIRAS3	2.56	RPAP3-DT	8.66	NEK10	3.33	NPFFR2	2.49
C3AR1	2.50	TSPAN11	8.14	TMEM265	3.33	CTXN1	2.49
IL33	2.50	SRGAP3	7.13	DPEP1	3.26	PTGS1	2.44
APLN	2.45	GOLGA8R	7.12	PKIB	3.26	MAFB	2.42
ADRA1D	2.21	LINC01303	6.65	NPTX2	3.17	ASS1	2.42
RGS5	2.10	LINC02159	6.52	KCNE3	3.17	CKB	2.41
CFI	2.08	DUT-AS1	6.30	RN7SL3	3.16	SLC9A7	2.40
SPTBN5	2.07	MAN1C1	6.10	SLC22A17	3.15	FOXD1	2.38
TGFA	2.01	ODAD3	6.07	BMPER	3.15	H2BC12	2.32
		CPE	5.98	H2BC5	3.07	ASRGL1	2.30
		KIF1A	5.85	ADAMTS18	3.04	CXADR	2.29
		PTGIS	5.56	IL2RB	3.02	SELL	2.26
		GRM1	5.52	AFTPH-DT	3.02	ZNF667-AS1	2.23
		MIR503HG	5.46	ADRA1D	2.96	INKA1	2.22
		AIF1L	5.31	HSD17B14	2.94	LINC02154	2.22
		PCDHB6	5.23	RNASE1	2.89	MAP1A	2.18
		SOGA3	4.88	PRND	2.82	SLC12A5	2.14
		MMP9	4.78	SLCO2B1	2.82	COL12A1	2.13
		MARVELD3	4.70	SORL1	2.81	KCNN4	2.13
		ZAP70	4.62	PIK3R3	2.78	ZC3H12A-DT	2.11
		CPA4	4.60	NPTXR	2.76	ADGRG4	2.10
		SNCB	4.45	WDFY4	2.75	TMEM163	2.06
		CPM	4.28	LIMCH1	2.75	MYG1-AS1	2.06
		SOGA3	4.00	APLN	2.71	RPLP0P6	2.04
		RGS5	3.93	CD36	2.71	CORO2B	2.04
		PCDH17	3.93	COL15A1	2.71	CETP	2.04
		PCMTD1-DT	3.93	OLFM1	2.71	CHST6	2.01
		H2BC4	3.79	DCLK1	2.68	HOXD3	2.00

Table S8. Gene set enrichment analysis comparisons between sh*Ctr*-HDLECs and sh*S1PR1*-HDLECs with CD4 T cell co-culture.

Gene Set Name	Genes in Gene Set (K)	Genes in Overlap (k)
CELL CELL SIGNALING	1679	18
CELL ADHESION	1541	16
CELLULAR_MONOVALENT INORGANIC ANION HOMEOSTASIS	11	3
CELL MOTILITY	1794	17
ANATOMICAL STRUCTURE FORMATION INVOLVED IN MORPHOGENESIS	1244	14
REGULATION OF CELLULAR LOCALIZATION	954	12
NEGATIVE REGULATION OF PROTEIN LOCALIZATION	203	6
CELLULAR ANION HOMEOSTASIS	20	3
MONOVALENT INORGANIC ANION HOMEOSTASIS	20	3
SYNAPTIC SIGNALING	761	10
CELLULAR HOMEOSTASIS	775	10
CENTRAL NERVOUS SYSTEM PROJECTION NEURON AXONOGENESIS	28	3
CELLULAR ION HOMEOSTASIS	517	8
LYMPHOCYTE ACTIVATION	841	10
PHOSPHORYLATION	1862	15
CELL VOLUME HOMEOSTASIS	32	3
LOCOMOTION	1446	13
CELL JUNCTION ORGANIZATION	707	9
T CELL ACTIVATION	549	8
CENTRAL NERVOUS SYSTEM NEURON DIFFERENTIATION	174	5

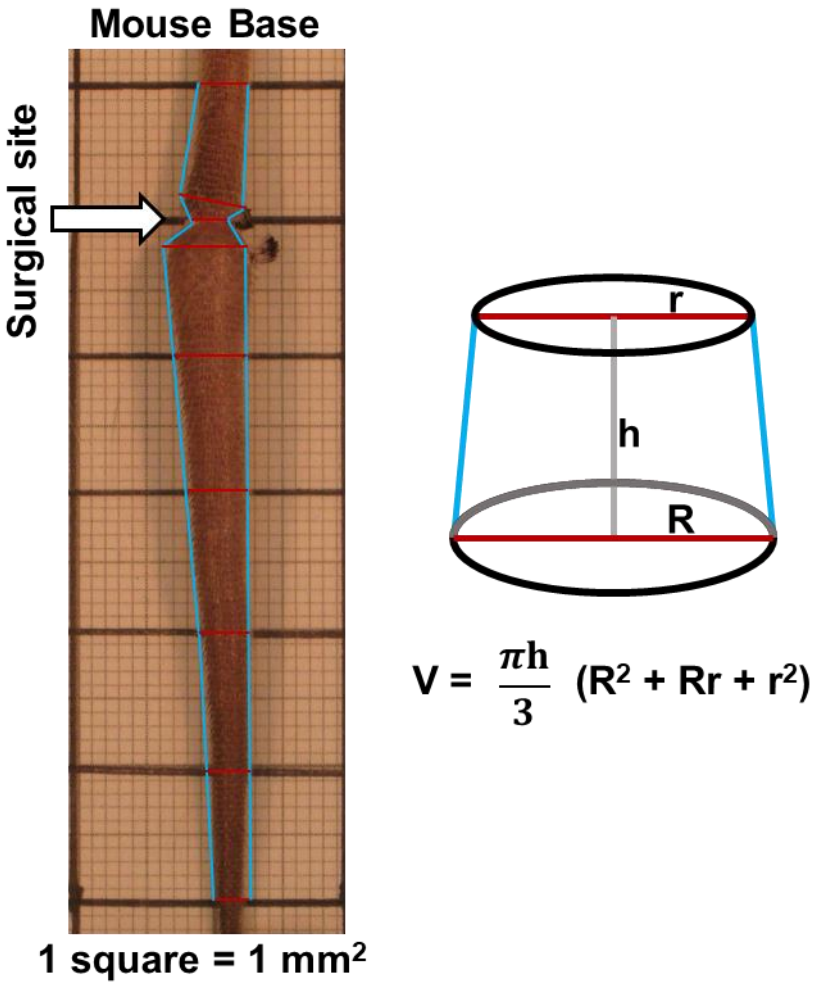

Figure S1. Tail volume was calculated through a digital photographic technique. Mouse-tail volume was calculated through a digital photographic technique pre-operatively, and post-operatively on d7, d14, and d21 using an Olympus D520 Zoom digital camera at SHQ resolution at a fixed distance from the subject (37cm). All images were processed and analyzed in Adobe Photoshop CS6.

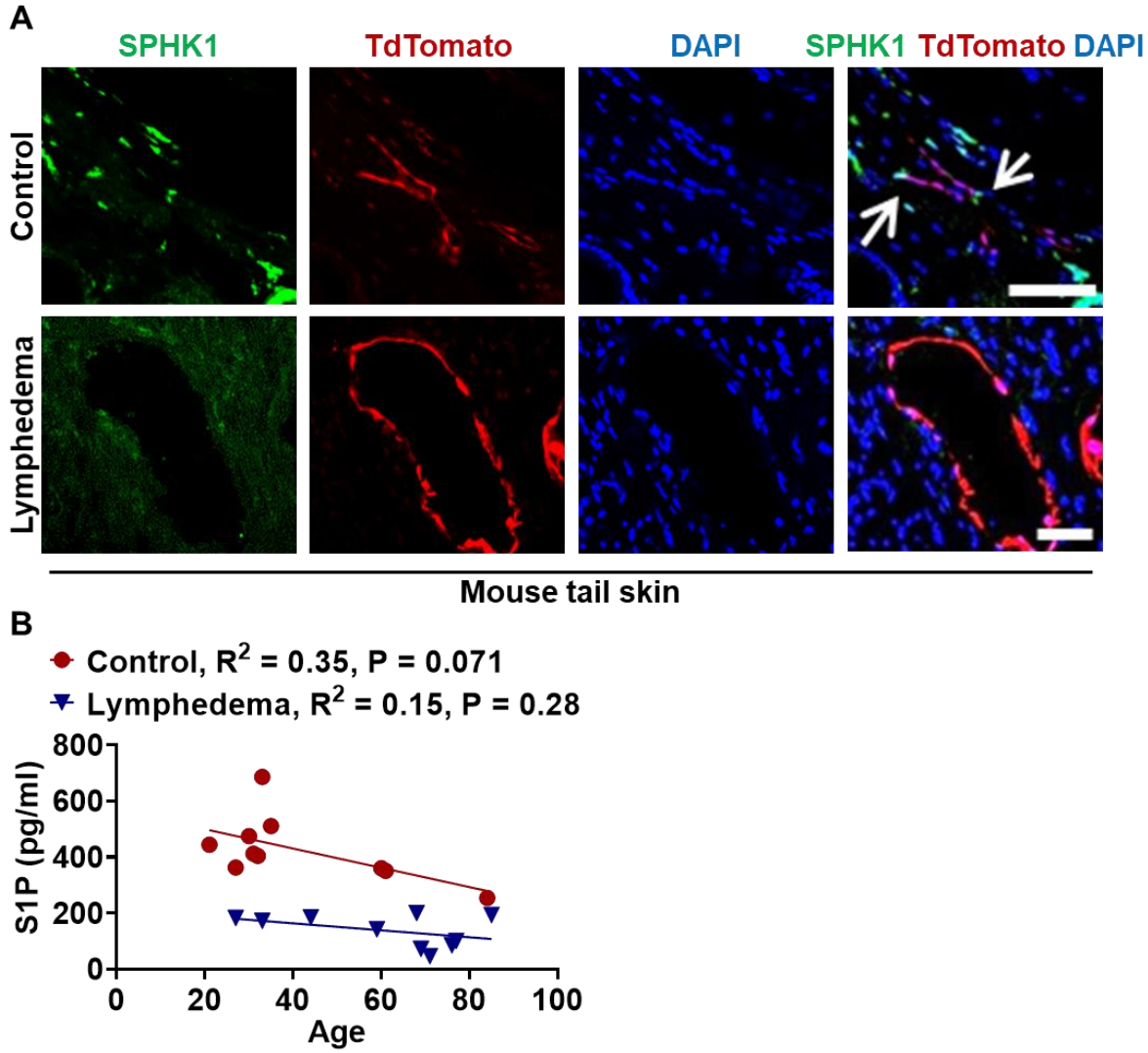

Figure S2. Decreased S1P signaling with lymphedema in both human and mouse. **(A)** Representative immunofluorescent staining of SPHK1 (green) in *Prox1-Cre^{ERT2}-tdTomato* mouse tail-skin. Tissues were harvested on d21 following sham surgery (control) or lymphedema surgery. DAPI (blue) stains nuclei; white arrows indicate co-staining; scale bar = 20μm. Note that different magnifications were used to better illustrate lymphatic structures in the control and lymphedema groups. **(B)** S1P concentrations were plotted against age of each individual. R^2 and P values were calculated by Pearson correlation test (n = 10 per each group). R^2 were calculated by Pearson correlation test.

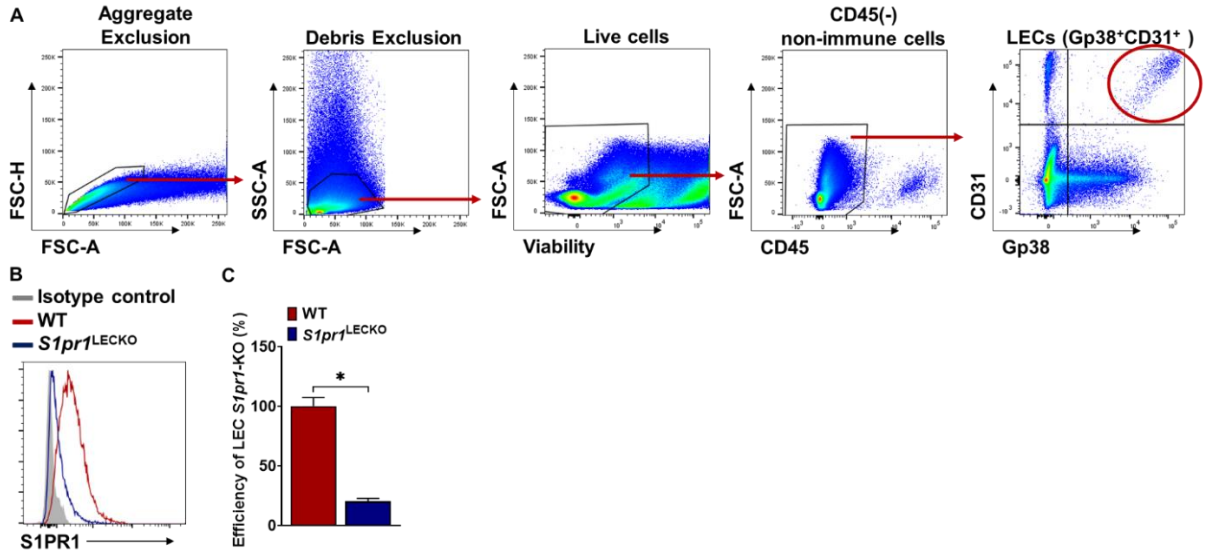

Figure S3. *Prox1-cre^{ERT2}* effectively mediates *S1pr1* deletion in LECs.
(A) Flow cytometric analysis was performed 3 weeks after tamoxifen treatment. Flow cytometric gating scheme for the determination of LEC population. The singlet is singe cell gating for doublet discrimination. **(B and C)** S1PR1 fluorescence intensity in LEC ($Gp38^+CD31^+$) in the tail skin from WT (red) and *S1pr1*^{LECKO} (blue) mice was quantified by flow cytometric analysis. Representative (B) and compiling data (C) are shown (n = 4 per each group). Data are presented as mean ± SEM; * $p < 0.05$ by the Mann-Whitney test.

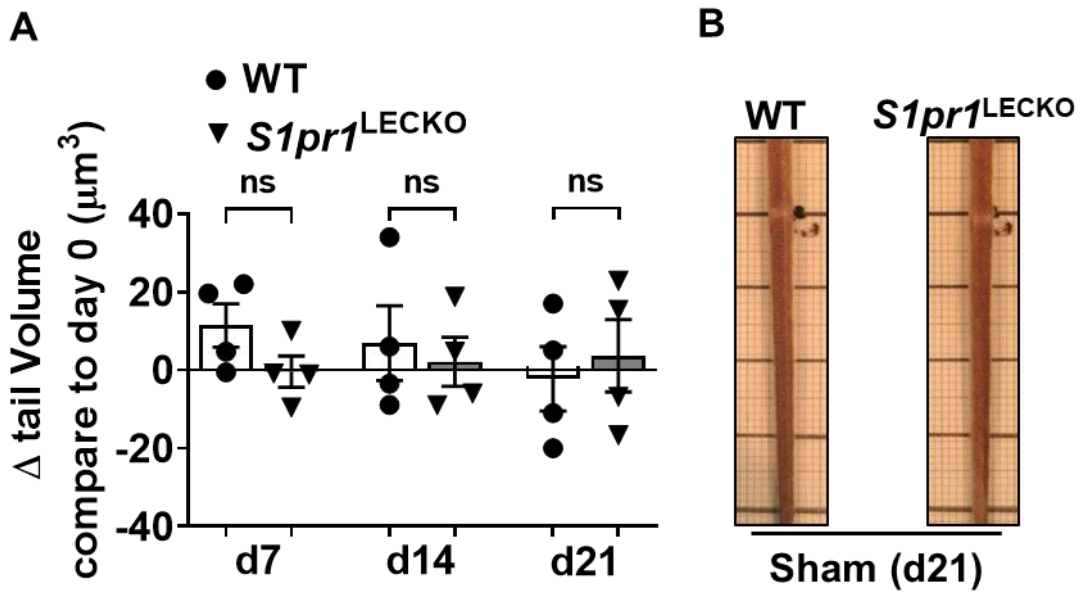

Figure S4. *S1pr1*^{LECKO} does not affect wound healing following sham surgery.
(A) Tail volume measurements of WT and *S1pr1*^{LECKO} on 7d, 14d, and 21d following sham surgery (n = 4 per each group). **(B)** Representative tail image 21d following sham surgery. Data are presented as mean ± SEM; ns (not significant) by the Mann-Whitney test.

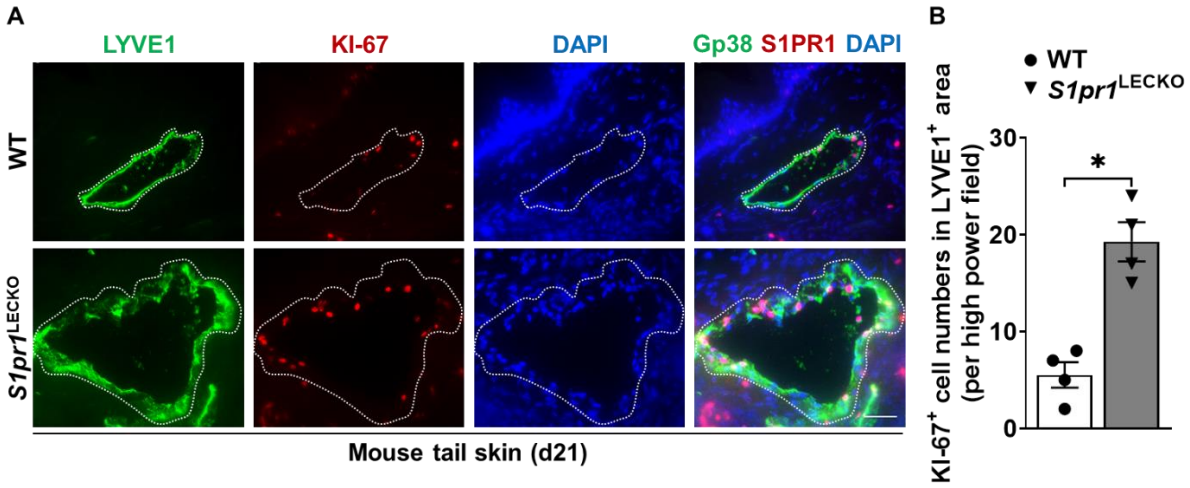

Figure S5. Increased KI-67$^+$ cells of LYVE1 area in lymphatic specific *S1pr1*-deficient lymphedema mice.

(A and B) Immunofluorescent images of LYVE1 (green) and KI-67 (red) of tail skin 21d after surgery. Representative image (A) and quantification KI-67$^+$ cells in the LYVE1 areas (B) are shown (n = 4 per each group). DAPI (blue) stains the nucleus. Scale bar = 50 μm. Data are presented as mean ± SEM; * $p < 0.05$ by the Mann-Whitney test.

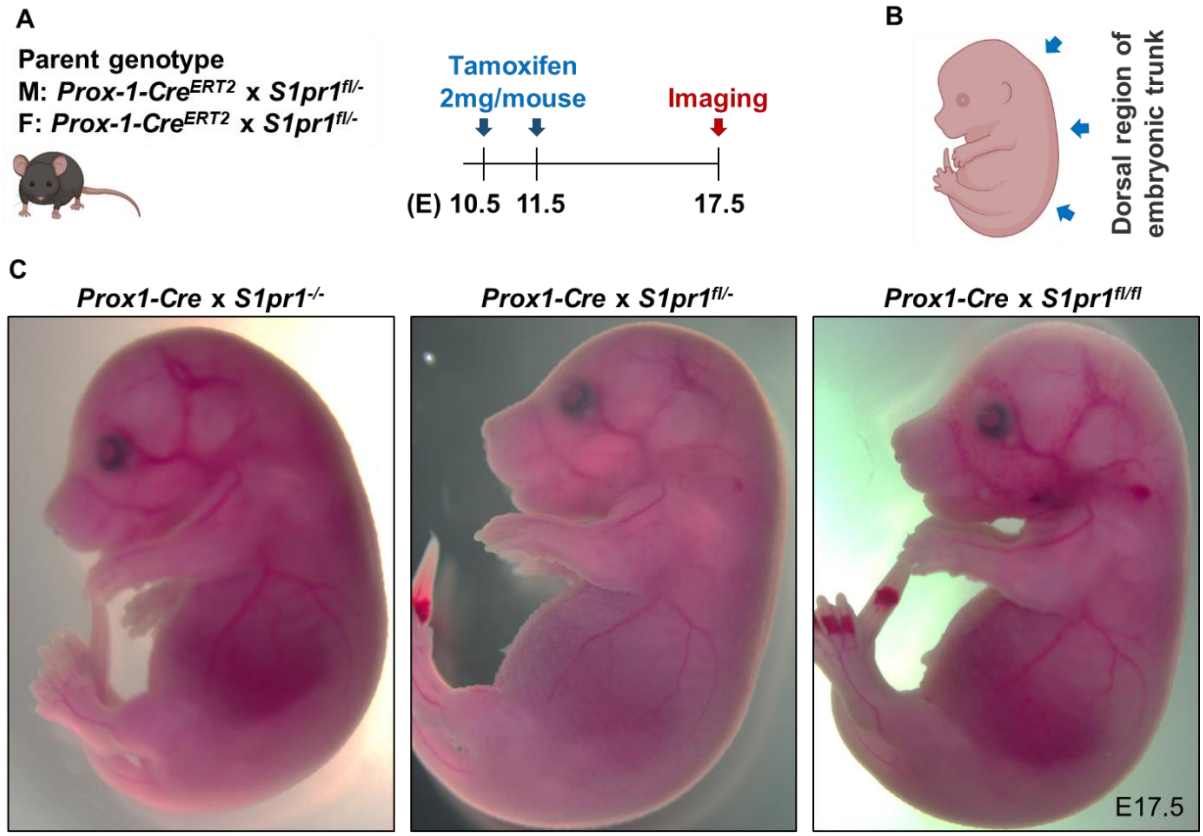

Figure S6. No dorsal edema pattern in mouse embryos lacking lymphatic specific *S1pr1*. **(A)** Strategy for injecting pregnant mice (*Prox-1-Cre*^{ERT2} x *S1pr1*$^{fl/-}$ mated with *Prox-1-Cre*^{ERT2} x *S1pr1*$^{fl/-}$) with tamoxifen. **(B)** Arrow shows edema formation observed in the dermis of the back. **(C)** Freshly harvested embryos in E17.5 were imaged under a brightfield microscope.

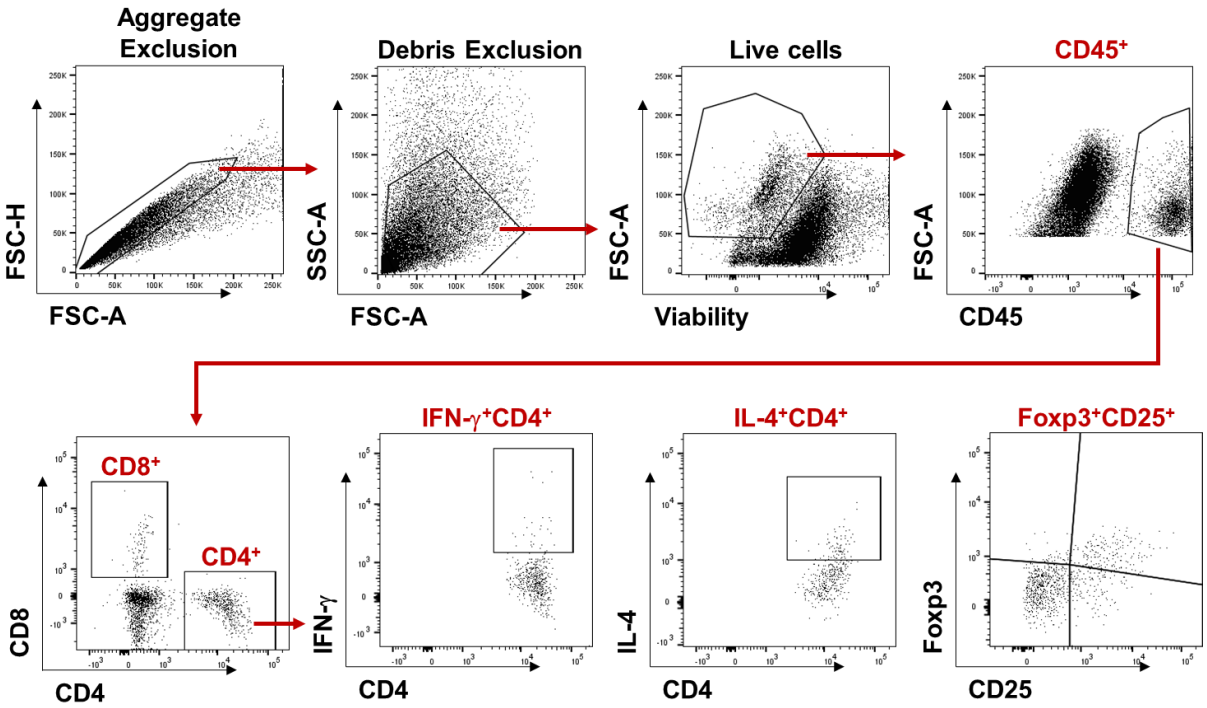

Figure S7. Flow cytometry analysis strategy for T cell population profiling in tail skin. Representative flow cytometric gating scheme for determining T cell populations in the tail skin. IFN-γ$^+$CD4$^+$ for Th1, IL-4$^+$CD4$^+$ for Th2, and Foxp3$^+$CD25$^+$ for Treg.

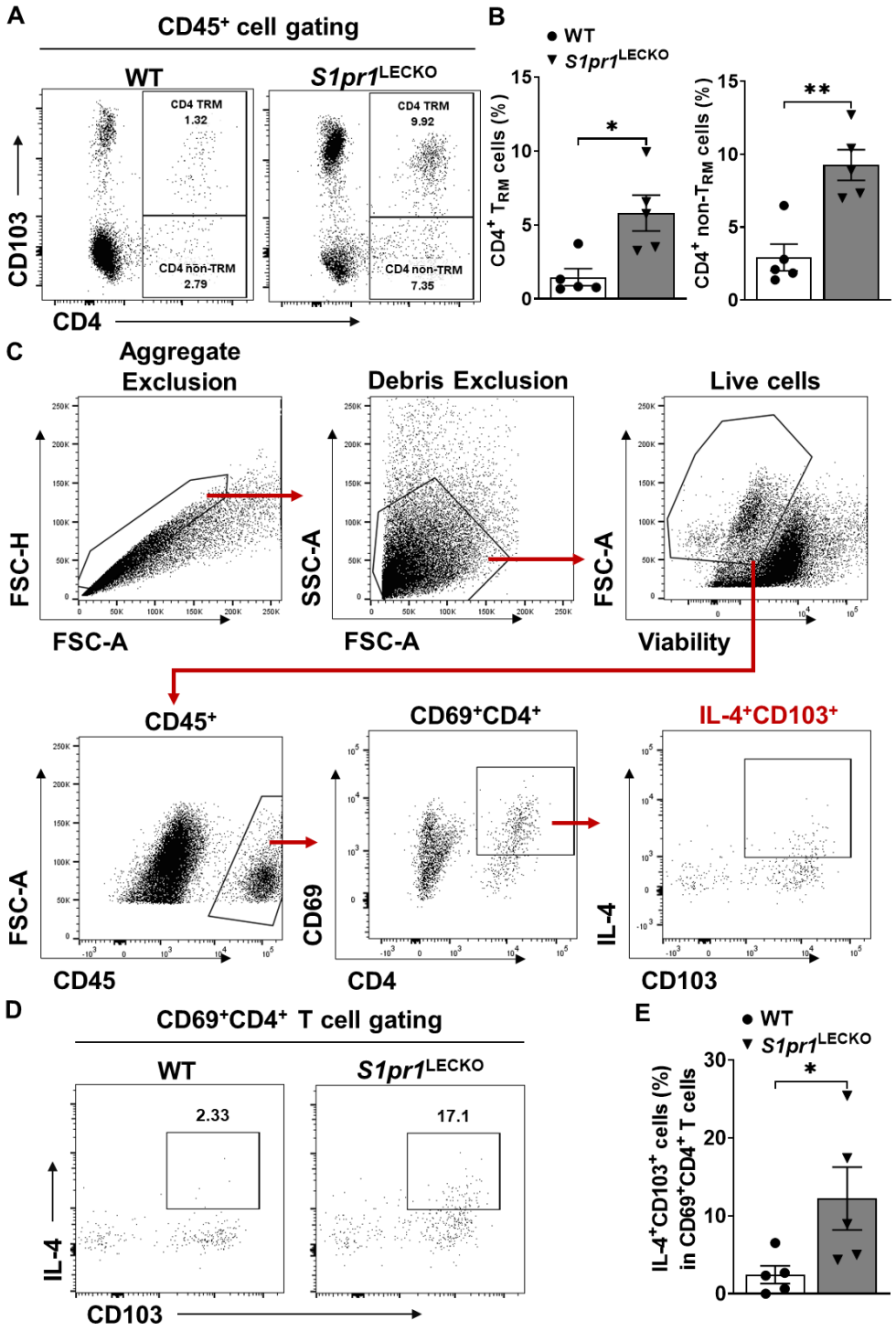

Figure S8. IL-4$^+$ tissue-resident T memory (T_{RM}) cells are increased in *S1pr1*^{LECKO} lymphedema mouse groups.

(A and B) Flow cytometric analysis was performed d21 after lymphatic surgery. Representative flow cytometric plots (A) and quantification (B) of CD103$^+$CD4$^+$ T_{RM} and CD103$^-$CD4$^+$ non-T_{RM} cells in tail tissue skin (n = 5 per each group). **(C)** Representative flow cytometric gating scheme for determining IL-4-producing T_{RM} cell populations in the tail skin. **(D and E)** Representative flow cytometric plots (D) and quantification (E) of IL-4$^+$CD103$^+$ in CD69$^+$CD4$^+$ T_{RM} cells in tail tissue skin (n = 5 per each group). Data are presented as mean ± SEM; * $p < 0.05$ and ** $p < 0.01$ by the Mann-Whitney test.

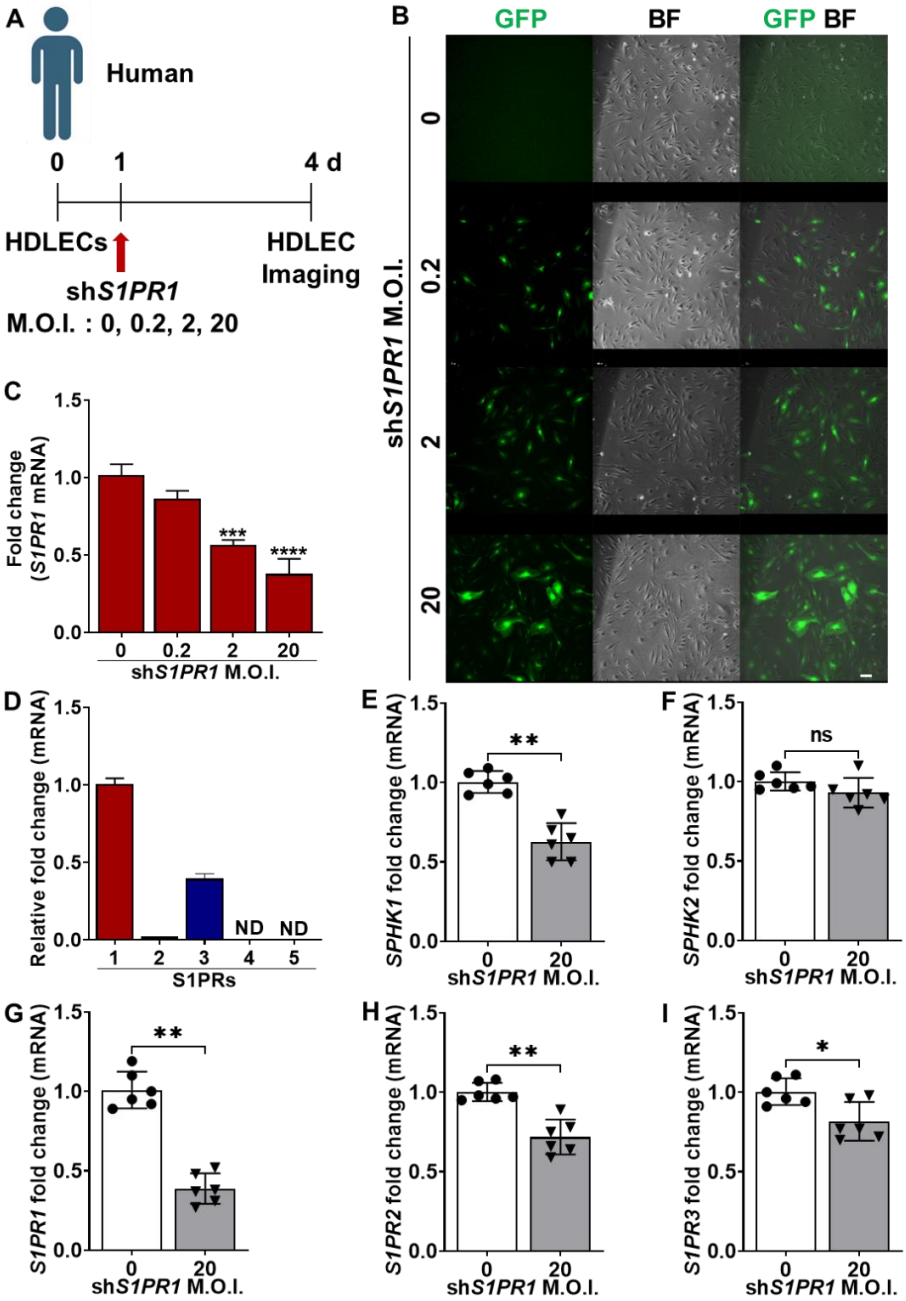

Figure S9. sh*S1PR1* trans-infection does not affect HDLEC viability and decreases S1PRs.

(A) Timeline of M.O.I.-dose dependent effects of sh*S1PR1* treatment on HDLECs. **(B)** Green fluorescent protein (GFP) tagged lentiviral sh*S1PR1*-treated HDLECs following 3 days of culture. GFP and brightfield (BF) were imaged with fluorescence microscopy. Scale bar = 100 µm. **(C)** *S1PR1* mRNA level of HDLECs were analyzed by using RT-qPCR (n ≥ 4 per each group). (D) Relative mRNA level of S1PRs family (S1PR1,2,3,4, and 5) on HDLECs by using RT-qPCR (n ≥ 4 per each group). **(E to I)** RT-qPCR analysis of *SPHK1* (E), *SPHK2* (F), *S1PR1* (G), *S1PR2* (H), *and S1PR3* (I) mRNA levels in S1PR1 knock-down HDLECs (n = 6 per each group). Data for C is presented as mean ± SEM; *** $p < 0.001$, and **** $p < 0.0001$ compared with the sh*Ctr* (M.O.I. = 0) by Ordinary one-way ANOVA. Data for E, F, G, H, and I are presented as mean ± SEM; ns (not significant), * $p < 0.05$, ** $p < 0.01$, and **** $p < 0.0001$ by the Mann-Whitney test. ND; not detected.

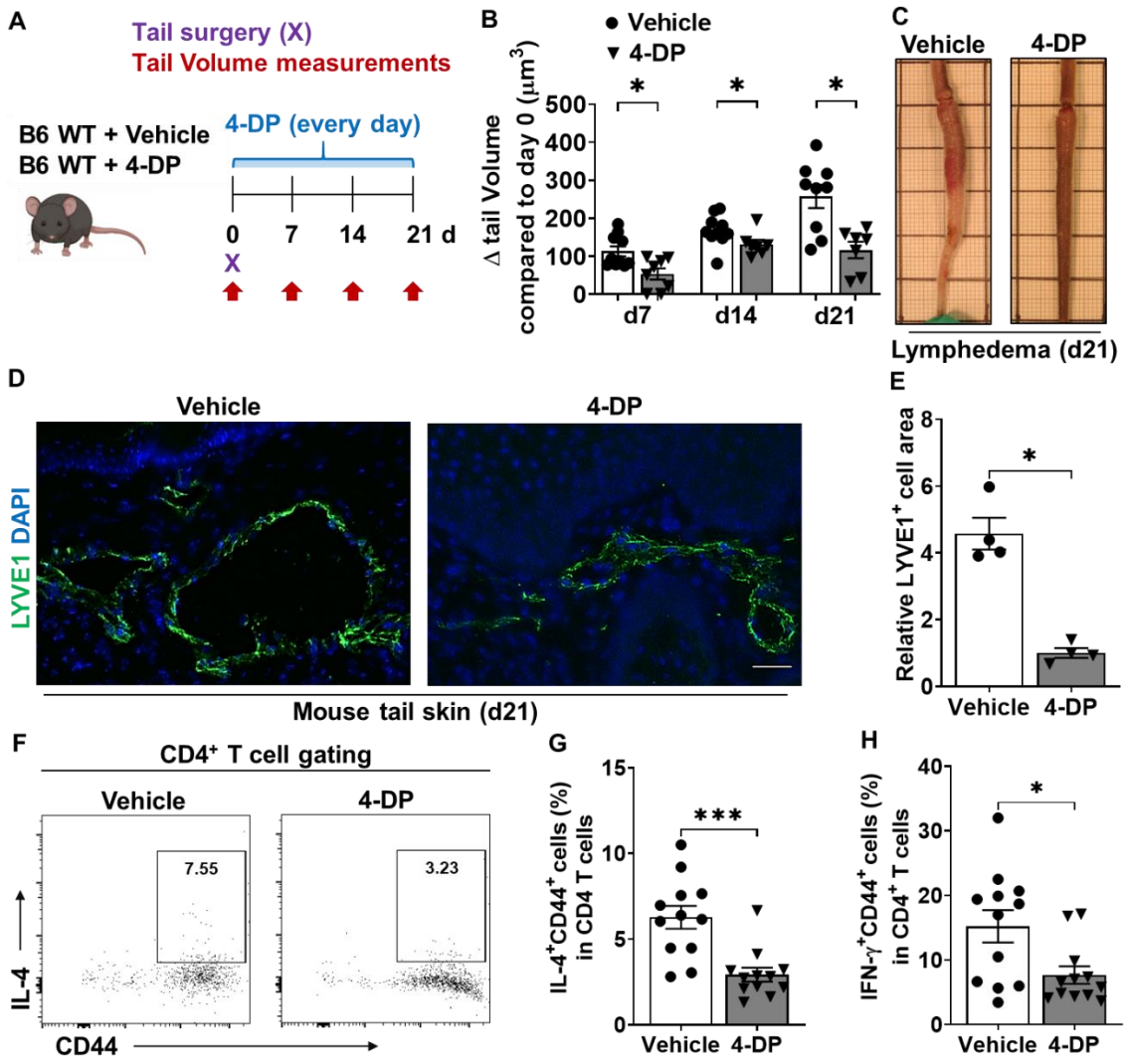

Figure S10. Increased S1P signaling alleviates lymphedema development.
(A) Schematic diagram of the experimental protocol. 10 mg/kg 4-DP or vehicle (PBS) was injected i.p. every day after tail surgery. **(B)** Quantification of tail volume changes over time of vehicle or 4-DP treated mice after lymphatic surgery (n ≥ 7 per each group). **(C)** Representative photographs of tails 21d following lymphatic surgery. **(D and E)** Immunofluorescent images of LYVE1 (green) of tail skin 21d after surgery. Representative image (D) and quantification of the LYVE1 areas (E) are shown (n = 4 per each group). DAPI (blue) stains the nucleus. Scale bar = 50 μm. **(F and G)** Flow cytometric analysis was performed d21 after lymphatic surgery. Representative flow cytometric plots (F) and quantification of IL-4$^+$CD44$^+$ in CD4$^+$ T cells in tail tissue skin (G) (n = 12 per each group). **(H)** quantification of IFN-γ$^+$CD44$^+$ in CD4$^+$ T cells in tail tissue skin (n = 12 per each group). Data are presented as mean ± SEM; * $p < 0.05$ and *** $p < 0.001$ by the Mann-Whitney test.

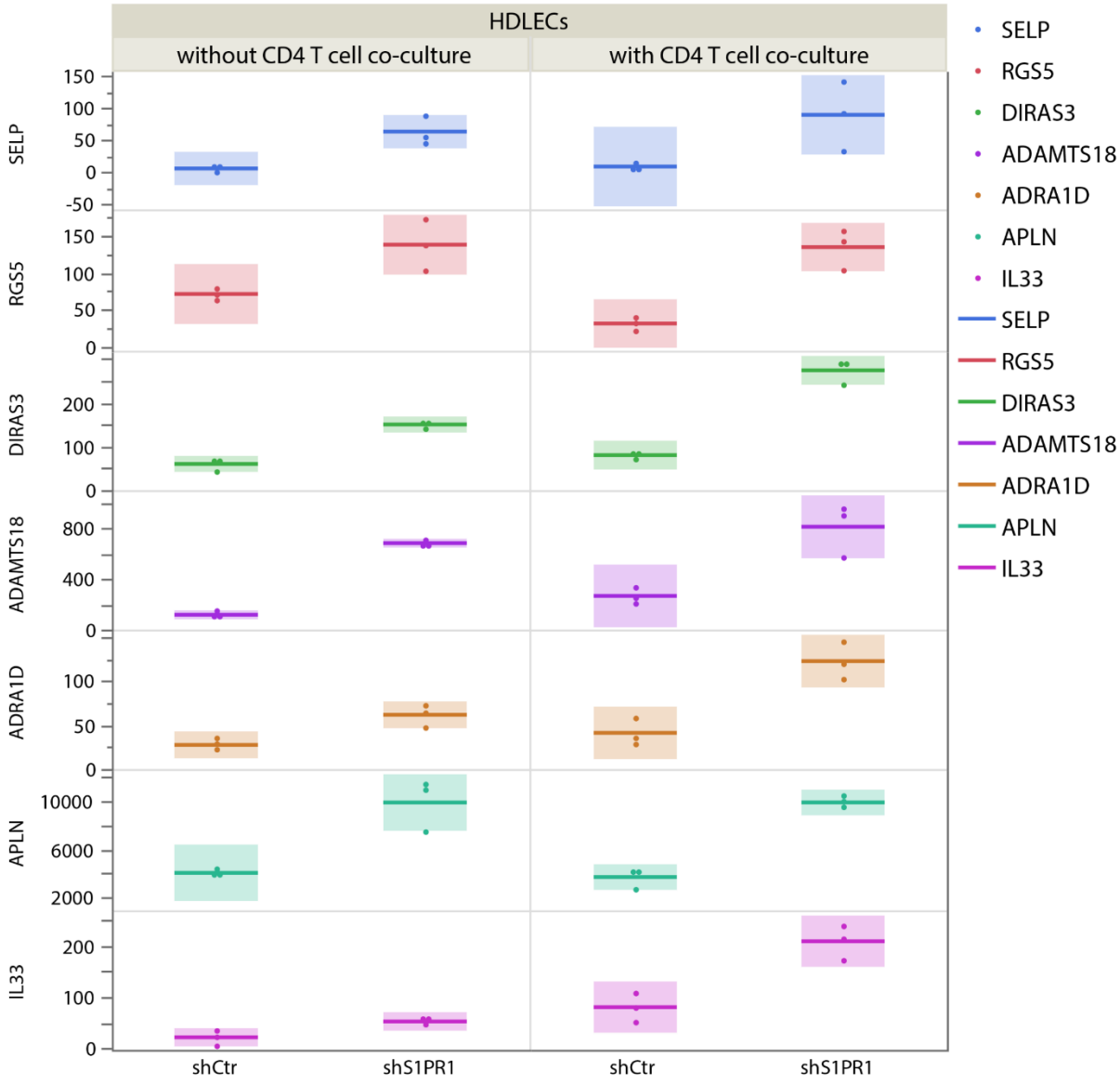

Figure S11. Differential expression gene (DEG) results for upregulated-overlapped 7 genes in S1PR1 knock-down HDLECs with and without CD 4 T cell co-culture.
Comparison of both upregulated and overlapped genes between sh*S1PR1* treated-HDLEC with and without CD4 T cell co-culture for 3day in the present of α-CD3/28 Abs using RNA-seq data.

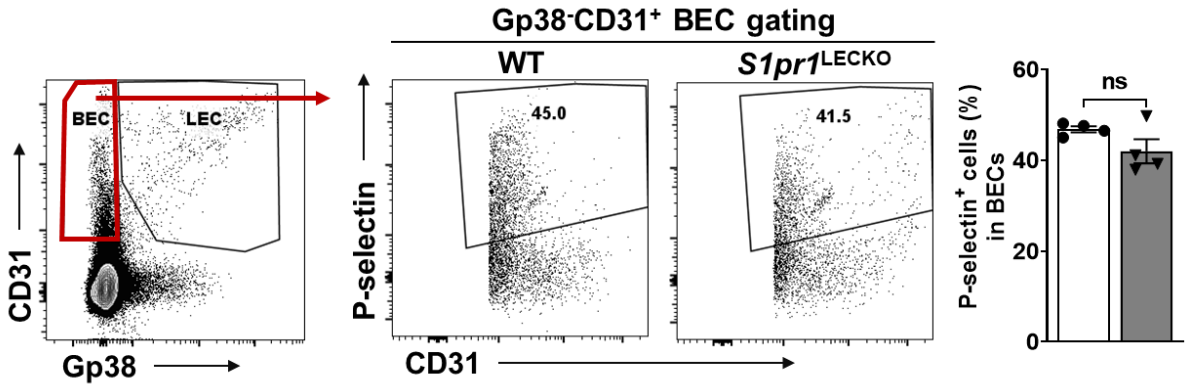

Figure S12. P-selectin^{+} BECs are not significantly different in lymphatic S1pr1-deficient mice.

Flow cytometric analysis was performed from the tail skin of WT and *S1pr1*^{LECKO} mice. Representative flow cytometric plots and quantification of P-selectin^{+} BECs in tail tissue skin (n ≥ 4 per each group). Data are presented as mean ± SEM; ns (not significant) compared with the WT group; by the Mann-Whitney test. BEC; Blood endothelial cell

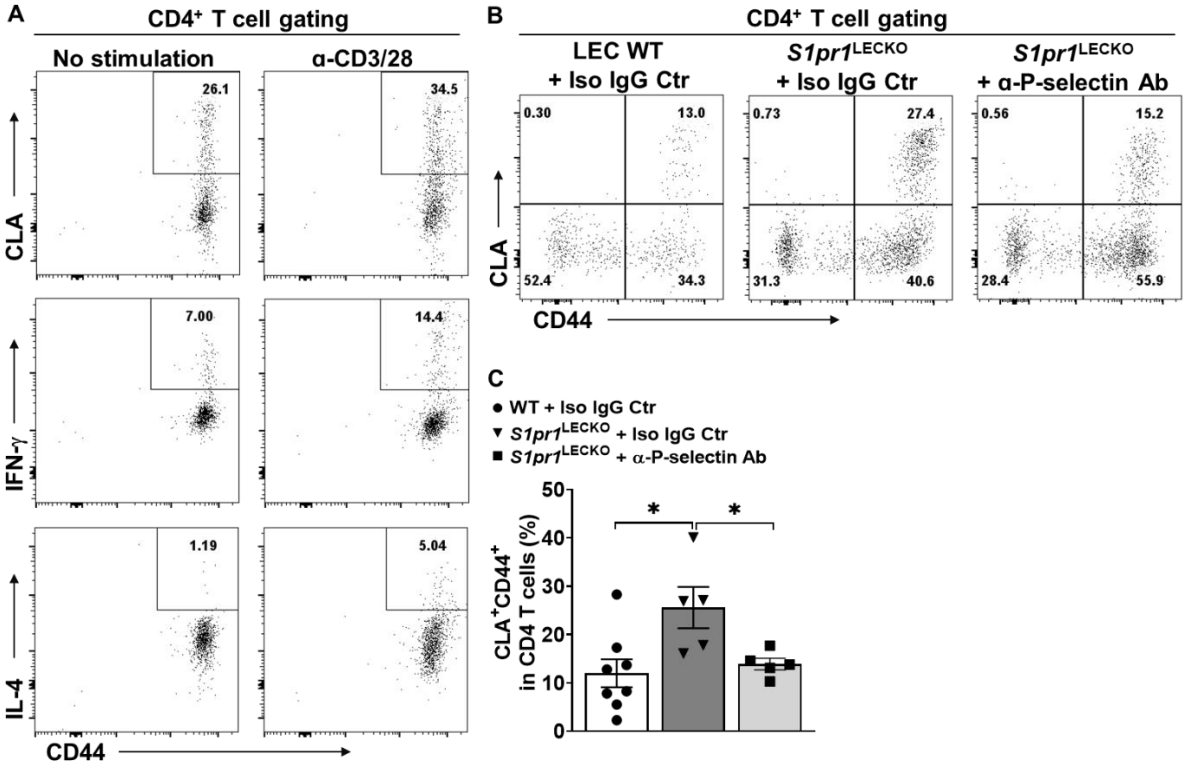

Figure S13. Decreased CLA$^+$CD4 T cell population in lymphedema tail skin after anti P-selectin Ab treatment.

(A) Memory CD4 T cells were isolated from PBMC and cultured with or without α-CD3/28 antibody for 3 days. Flow cytometric plots of CLA$^+$, IFN-γ$^+$, and IL-4$^+$ CD44$^+$ in CD4$^+$ T cells were shown. **(B and C)** Representative flow cytometric plots (B) and quantification (C) of CLA$^+$CD44$^+$ in CD4$^+$ T cells in tail skin. Data are presented as mean ± SEM; * $p < 0.05$ compared with the *S1pr1*^{LECKO} + Iso Ctr group; by the Ordinary one-way ANOVA.

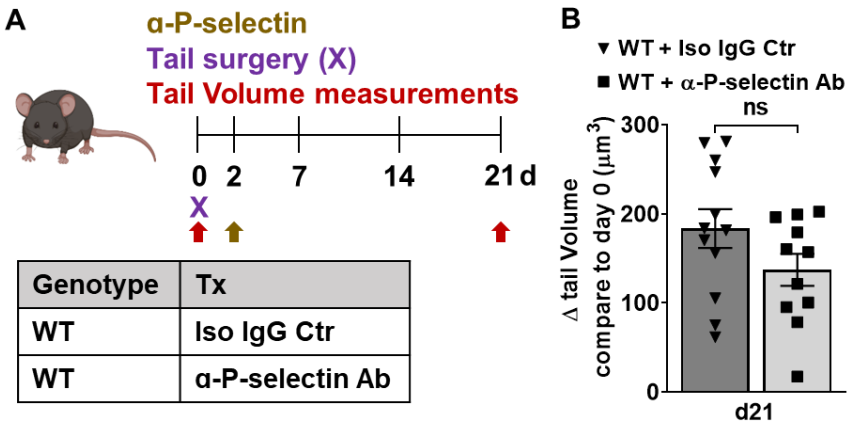

Genotype	Tx
WT	Iso IgG Ctr
WT	α-P-selectin Ab

Figure S14. α-P-selectin injection 2 days after lymphedema surgery shows trend of decreased tail swelling but is not statistically significant.
(A) Schematic diagram of the experimental protocol. Schematic diagram of the experimental protocol. 5 mg/kg anti-mouse P-selectin Ab (RB40.34.4) or Isotype IgG control (Iso IgG Ctr) was retro-orbital-i.v. injected into WT mice 2 days after lymphedema surgery and the tail size of animals was measured at day 21. **(B)** Quantification of tail volume changes of tail skin on day 21 after surgery (n ≥ 11 per each group. Data are presented as mean ± SEM; ns (not significant) compared with the *S1pr1*^{LECKO} + Iso Ctr group; by the Mann-Whitney test.